Universality in network dynamics

Baruch Barzel[1,2] and **Albert-László Barabási**[1,2,3]

[1]Center for Complex Network Research and Departments of Physics, Computer Science and Biology, Northeastern University, Boston, Massachusetts 02115, USA

[2]Center for Cancer Systems Biology, Dana-Farber Cancer Institute, Harvard Medical School, Boston, Massachusetts 02115, USA

[3]Department of Medicine, Brigham and Women's Hospital, Harvard Medical School, Boston, Massachusetts 02115, USA

Abstract

Despite significant advances in characterizing the structural properties of complex networks, a mathematical framework that uncovers the universal properties of the interplay between the topology and the dynamics of complex systems continues to elude us. Here we develop a self-consistent theory of dynamical perturbations in complex systems, allowing us to systematically separate the contribution of the network topology and dynamics. The formalism covers a broad range of steady-state dynamical processes and offers testable predictions regarding the system's response to perturbations and the development of correlations. It predicts several distinct universality classes whose characteristics can be derived directly from the continuum equation governing the system's dynamics and which are validated on several canonical network-based dynamical systems, from biochemical dynamics to epidemic spreading. Finally, we collect experimental data pertaining to social and biological systems, demonstrating that we can accurately uncover their universality class even in the absence of an appropriate continuum theory that governs the system's dynamics.

I. Introduction

Despite the profound diversity in the scale and purpose of networks observed in nature and technology, their topology shares several highly reproducible and often universal characteristics [1–8]: many real networks display the small world property [9], are scale-free [10], develop distinct community structure [11], and show degree correlations [12, 13]. Yet, when it comes to the dynamical processes that take place on these networks, diversity wins over universality [14–16]. To be sure, advances in our understanding of synchronization [17, 18], spreading processes [19–21] or spectral phenomena [22] have offered important clues on the interplay between network topology and network dynamics. We continue to lack, however, a general predictive framework that can treat a broad range of dynamical models using a unified theoretical toolbox. Indeed, currently each network-based dynamical process, from reaction dynamics in cellular metabolism to the spread of viruses in social networks, is studied on its own terms, requiring its dedicated analytical formalism and numerical tools. This diversity of behavior raises a fundamental question: are there common patterns in the dynamics of various complex systems? Alternatively, could the current diversity of

modeling platforms and dynamical characteristics reflect an inherent and ultimately unbridgeable gulf between different dynamical systems?

We illustrate the depth of this problem by focusing on the dynamics of a system with N components (nodes), where each node i is characterized by an *activity* $x_i(t)$, following

$$\frac{dx_i}{dt} = W\left(x_i(t)\right) + \sum_{j=1}^{N} A_{ij} Q\left(x_i(t), x_j(t)\right), \quad (1)$$

providing a rather general deterministic description of systems governed by pairwise interactions. The first term on the r.h.s. of (1) describes the self-dynamics of x_i, accounting for processes like influx, degradation or reproduction. The second captures i's interactions with its neighbors, in which A_{ij} is the adjacency matrix and $Q(x_i, x_j)$ describes the *dynamical mechanism* governing the pairwise interactions. With the appropriate choice of the nonlinear $W(x_i)$ and $Q(x_i, x_j)$ Eq. (1) can be mapped exactly into several dynamical models explored in the literature (Table I), like (a) epidemic processes ($\mathcal{E}$), where x_i represents the probability of infection [23–25], (b) biochemical dynamics ($\mathcal{B}$), in which x_i represents the concentration of a reactant [26–29] (c) birth-death processes ($\mathcal{BD}$) [30–32], in which x_i represents the population at site i and (d) regulatory dynamics ($\mathcal{R}$) in which x_i is the expression level of a gene [33, 34].

The traditional probing of the dynamics of a complex system is achieved through perturbation experiments, that explore changes in the activity x_i of node i in response to changes induced in the activity of node j. Hence we focus on the system's linear response by inducing a permanent perturbation dx_j on the steady state activity x_j and following the subsequent changes in all x_i through the *correlation matrix* [28] (Secs. S.II and S.VI)

$$G_{ij} = \frac{dx_i/x_i}{dx_j/x_j}. \quad (2)$$

In biology G_{ij} represents the impact of a perturbed gene j on a target gene i; in social systems G_{ij} captures the influence of an individual j on i. There is ample empirical evidence from gene expression [35–39] to metabolism [40] and neuronal systems [41] that the distribution of pairwise node-node correlations, or $P(G_{ij})$, is fat tailed, a phenomena that lacks quantitative explanation. Our measurements support this: we obtained G_{ij} for the four dynamical systems described in Table I, in each case finding that $P(G) \sim G^{-\nu}$ (Figs. 1a1 - a4 and S5a1 - a3). We find systematic differences in ν, however: for $\mathcal{B}$ and $\mathcal{BD}$ $\nu = 2$ and for $\mathcal{R}$ and ε $\nu = 3/2$. We also find that the distribution $P(G)$ is independent of the nature of the underlying network (scale-free, Erdős-Rényi or networks provided by experimental data), suggesting that ν is determined only by the dynamical laws that govern these systems.

To obtain a more detailed understanding of a system's response to perturbations, we also explored several other frequently pursued dynamical measures.

Impact and stability

We define *i*'s *impact* as

$$I_i = \sum_{j=1}^{N} A_{ij} G_{ij}^{\mathrm{T}}, \quad (3)$$

capturing the average response of *i*'s neighborhood to *i*'s perturbation. Similarly, we define *i*'s *stability* as

$$S_i = \frac{1}{\sum\limits_{j=1}^{N} A_{ij} G_{ij}}, \quad (4)$$

in which the denominator captures the magnitude of *i*'s response to individual perturbations of *i*'s nearest neighbors. If *i* responds strongly to neighboring perturbations, then S_i is small, indicating that node *i* is unstable. Hence I_i captures the influence of node *i* on its neighborhood, while S_i captures the inverse process, the neighborhood's influence on *i*. In Figs. 1b1 - c4 and S5b1 - c3 we show the stability and impact distributions, $P(S)$ and $P(I)$, for the four dynamical models, finding a seemingly inconsistent behavior: for ε $P(S)$ and $P(I)$ are bounded when $P(k)$ is bounded (Erdős-Rényi) and fat-tailed when $P(k)$ is fat-tailed (scale-free); for $\mathcal{BD}$ $P(I)$ follows a similar behavior, but $P(S)$ is always bounded, regardless of $P(k)$; for $\mathcal{B}$ and $\mathcal{R}$ both $P(S)$ and $P(I)$ are always bounded.

Propagation

In a network environment a perturbation does not stay localized, but can reach distant nodes. To track the spread of perturbations we use the distance dependent correlation function [27–29]

$$\Gamma(l) = \frac{1}{N} \sum_{j=1}^{N} \sum_{i \in K_j(l)} G_{ij}, \quad (5)$$

where $K_j(l)$ is the group of all nodes at distance *l* from *j*. Equation (5) describes the magnitude of the perturbations experienced by *all* nodes at distance *l* from the source. The decay rate of $\Gamma(l)$ determines whether perturbations penetrate the network or remain localized in the source's vicinity. We find that for $\mathcal{B}$ and $\mathcal{BD}$ $\Gamma(l)$ shows no decay, documenting a *conservative* process in which the original perturbation propagates without loss, a phenomena well documented in [27–29]. For $\mathcal{R}$ and ε we observe *dissipation*, where perturbations decay exponentially as they penetrate the network (Figs. 1d1 - d4 and S5d1 - d3).

Global cascades

The cascade size C_i represents the number of target nodes whose activity changes beyond a threshold following a perturbation of node *i*. A cascade can include all genes whose

expression levels significantly changed following a genetic perturbation or all individuals who adopt an innovation. The distribution of cascade sizes induced by perturbations, $P(C)$, is frequently measured in social [42–44] technological [45, 46] and biological [41, 47] systems, finding that $P(C)$ is often fat-tailed, an observation whose origins remain unclear. Our simulations (Figs. 1e1 - e4 and S5e1 - e3) indicate that $P(C)$ depends on the interplay between the topology and dynamics: for $\mathcal{BD}$, $\mathcal{R}$ and $\mathcal{E}$ $P(C)$ is driven by $P(k)$, hence these systems develop *heterogeneous* cascades with a fat-tailed $P(C)$ on a scale-free network but a bounded $P(C)$ on a random network. Protein dynamics ($\mathcal{B}$), however, has *uniform* cascades, characterized by a bounded $P(C)$, independent of the network topology.

Together the four functions discussed above provide a comprehensive description of the system's behavior, capturing local dynamics (S_i, I_i), propagation to distant nodes ($\Gamma(l)$) and the global response of the system to perturbations (C_i). Yet, they also illustrate the rather diverse dynamical behaviors Eq. (1) can generate, capturing the true diversity in the response to perturbations observed in real systems. While these differences are clearly encoded somehow in the functional form of $W(x_i)$ and $Q(x_i, x_j)$ in (1), currently we have no way of predicting how a system responds to perturbations from the analytical formulation of the underlying dynamics. Hence our goal here is to develop an analytical formalism that bridges the structure of (1) and the diverse dynamical outcomes documented in Fig. 1. We focus on dynamics for which we can factorize $Q(x_i, x_j)$ as

$$\frac{Q(x_i, x_j)}{W(x_i)} = f(x_i)g(x_j), \quad (6)$$

in which $f(x_i)$ describes the impact of i's activity on itself and $g(x_j)$ describes the impact of i's neighbors on x_i. (A discussion of the expected behavior for systems that do not obey (6) is offered in Sec. S.VI). We show that the leading terms of these two functions, as expressed by the Laurent expansions

$$f^{-1}(x) = \sum_{n=-\infty}^{\infty} a_n x^n \quad (7)$$

and

$$g(f^{-1}(x)) = \sum_{m=-\infty}^{\infty} b_m x^m, \quad (8)$$

where $f^{-1}(x)$ is the inverse function of $f(x)$, uniquely determine the dynamics of the system (1) around its steady state and allow us to analytically predict each of the dynamical characteristics documented in Fig. 1. As only a small number of leading terms controls the expansions (7) and (8), we predict the existence of several broad universality classes that govern network dynamics. Finally, by demonstrating the validity of our results for two experimentally collected datasets, we offer evidence of a deep universality in network dynamics that crosses particular domains of inquiry.

II. Local Dynamics: Stability and Impact

We start by inducing a small perturbation, dx_j, around the steady state solution of (1), allowing us to write the response of j's nearest neighbor i as (Sec. S.III.A - B)

$$G_{ij} \sim \frac{x_j f(x_i)}{k_i x_i} \left(\frac{dg}{dx_j} \right) \left(\frac{df}{dx_i} \right)^{-1}, \quad (9)$$

where $x_i \sim f^{-1}(1/k_i)$ ($x_j \sim f^{-1}(1/k_j)$) is the steady state activity of i (j). For large k_i (k_j) G_{ij} will be dominated by the leading terms of (7) and (8). Denoting the leading terms of (7) and (8) by n_0 and m_0 respectively, and the leading *non-vanishing* terms by n_1 and m_1, we show that S_i (4) and I_i (3) depend on node i's degree as (Sec. S.III.C - D)

$$S_i \sim k_i^{\delta} \quad (10)$$

$$I_i \sim k_i^{\varphi}, \quad (11)$$

where $\delta = n_1 - n_0$ and $\varphi = \delta - m_1 + 1$. The value of δ allows us to identify two dynamical universality classes:

Uniform stability (δ = 0, Fig. 2a)

If in (7) $n_1 = n_0$, we have $\delta = 0$ in (10), and the stability of a node is independent of its degree, implying that hubs and less connected nodes respond similarly to perturbations in their immediate vicinity.

Heterogeneous stability (δ > 0, Fig. 2b)

The only other possibility is that $n_0 = 0$ and $n_1 > 0$ in (7), predicting $\delta = n_1$. Since $\delta > 0$, according to (10) hubs are more stable to local perturbations than small nodes. In other words, the higher the degree of a node, the less responsive it is to changes in its immediate neighborhood.

These dynamical universality classes determine the shape of $P(S)$. For uniform stability ($\delta = 0$) S_i is independent of k_i, hence $P(S)$ is independent of the degree distribution, $P(k)$. Thus $P(S)$ is bounded, independently whether $P(k)$ is scale-free or Poisson, hence all nodes have comparable dynamical stability (Fig. 2a). In contrast, for heterogeneous stability ($\delta > 0$), S_i increases with k_i, hence if $P(k)$ is fat-tailed, then $P(S)$ will be also fat-tailed (Fig. 2b). Table I lists δ derived for the four dynamical models, predicting $\delta = 0$ for $\mathcal{B}$, $\mathcal{BD}$ and $\mathcal{R}$ (Fig. 2a1 - a3), and $\delta = 1$ for $\mathcal{E}$ (Fig. 2b1). These predictions are in excellent agreement with the observed $P(S)$, depending on $P(k)$ for $\delta > 0$ and being independent of $P(k)$ for $\delta = 0$ (Fig. 1c1-c4).

The value of φ in (11) predicts two additional dynamical universality classes:

Uniform impact ($\varphi = 0$, Fig. 2c)

If $\phi = 0$ in (11), the local impact (3) is degree independent, hence a node's perturbation has roughly the same impact on its neighbors, regardless of whether the perturbed node is a hub or a peripheral node. In this case $P(I)$ is bounded, regardless of the degree distribution $P(k)$. Table I indicates that $\mathcal{B}$ and $\mathcal{R}$ belong to this universality class, hence for these models $I_i \sim k_i^0$ (Fig. 2c1 - c2) and $P(I)$ is bounded as predicted (Fig. 1b1 and b3).

Heterogeneous impact ($\varphi \neq 0$, Fig. 2d)

In this case the impact of a node is affected by its degree, hubs having a stronger (weaker) impact on the network when $\phi > 0$ ($\phi < 0$). Therefore $P(I)$ depends on $P(k)$, being fat-tailed if $P(k)$ is fat-tailed and bounded if $P(k)$ is bounded. This universality class includes $\mathcal{BD}$ ($\phi = 3/2$) and $\mathcal{E}$ ($\phi = 1$), as confirmed by Figs. 2d1 - d2 and 1b2 and b4.

For scale-free networks we also predict the specific form of $P(I)$ and $P(S)$ (Sec. S.VII.E), showing a perfect agreement with the simulations (Fig. 1b2, b4 and c4, red solid lines).

Taken together, we predict that the exponents δ and ϕ (11) and hence the behavior of $P(S)$ and $P(I)$, characterizing the system's local response to perturbations, are determined only by the functional form of $f(x)$ and $g(x)$. Consequently, δ and ϕ are independent of the system's topology and of the microscopic details of the dynamical equation (1). Together they determine four dynamical universality classes that can fully account for the diverse dynamical behavior observed though $P(S)$ and $P(I)$ in Fig. 1b1 - c4.

III. Propagation: Conservative vs. Dissipative Dynamics

We now turn to the propagation of perturbations, deriving $\Gamma(l)$ (5) for large networks ($N \rightarrow \infty$) with an arbitrary degree-distribution $P(k)$. In such networks the number of nodes at distance l from a node follows [5]

$$|K(l)| \sim e^{\alpha l}, \quad (12)$$

where

$$e^{\alpha} = \frac{\langle k^2 \rangle - \langle k \rangle}{\langle k \rangle} \quad (13)$$

is the average nearest neighbor degree. For networks satisfying (12), for $l < \langle l \rangle$ (Sec. S.IV)

$$\Gamma(l) = e^{-\beta \alpha l} \quad (14)$$

where $\beta = m_1 - m_0$ up to a logarithmic correction, which depends on microscopic details of (1), *e.g.* rate constants (see Sec. S.IV.E). While α is determined by the network topology, the *dissipation rate* β is determined solely by the dynamics through the expansion (8), resulting in two distinct dynamical behaviors:

Conservative dynamics (β = 0, Fig. 3b)

If the leading term in (8) is m_0 0 we have $m_1 = m_0$, predicting $\beta = 0$, and $\Gamma(l) = 1$. Hence the total magnitude of a local perturbation is sustained as it propagates through the network, describing a *conservative process*. In this case the individual correlations G_{ij} will decay with l, but this decay is driven entirely by the topological expansion of the network (12), distributing the original perturbation over an exponentially increasing number of nodes. Taking $g(x)$ and $f(x)$ from Table I we predict that $\mathcal{B}$ and $\mathcal{BD}$ belong to this universality class, as confirmed by the non-decaying $\Gamma(l)$ in Fig. 1d1 - d2.

Dissipative dynamics (β > 0, Fig. 3c)

If the leading term in (8) is $m_0 = 0$, we have $\beta = m_1 > 0$. This implies an exponential decay of $\Gamma(l)$, describing a *dissipative process*. Now the decay of G_{ij} has two origins: the dissipation of the perturbation and its distribution over an exponentially growing number of nodes. Such dissipative propagation is predicted for $\mathcal{R}$ and $\mathcal{E}$, both with $\beta = m_1 = 1$ (Table I), in perfect agreement with the results of Fig. 1d3 - d4 (solid lines).

These two universality classes also determine the distribution of pairwise correlations, $P(G)$ (Fig. 1a1 - a4). Using the fact that the average individual correlation at l is $G(l) = \Gamma(l)/K(l)$, we can write $P(G)dG = P[l(G)] \, (dl/dG)dG$, where $P(l) \sim e^{al}$ is the probability that a randomly selected node pair is at distance l. According to (14) and (12) $l(G) \sim -\ln G/(\beta + 1)a$, so $P(G)$ follows (Sec. S.IV.D)

$$P(G) \sim G^{-\nu}, \quad (15)$$

where

$$\nu = 1 + \alpha\lambda = \frac{\beta+2}{\beta+1}. \quad (16)$$

For conservative dynamics ($\beta = 0$) we have $\nu = 2$, and for dissipative dynamics ($\beta > 0$) we have $1 < \nu < 2$, where the smaller is ν, the stronger is the dissipation. Equation (16) predicts $\nu = 2$ for $\mathcal{B}$ and $\mathcal{BD}$ ($\beta = 0$), and $\nu = 3/2$ for $\mathcal{R}$ and $\mathcal{E}$ ($\beta = 1$), in perfect agreement with Fig. 1a1 - a4.

Equations (14) - (16) uncover the dependence of the correlation function on the network topology (a) and the dynamics (β), and their impact on the distribution of the pairwise correlations (ν). Like δ and ϕ, the value of β and ν is universal, being independent of the topology and the microscopic details of (1). Note that we can measure $P(G)$ without knowing the network topology, hence we can use (16) to obtain β and $\Gamma(l)$ (14) even if we lack a map of the system, a result of strong empirical importance as for many systems of interest we lack an accurate network map (see Sec. S.IX.A).

IV. Global Dynamics: Cascades

Our analysis up to this point revealed two independent universalities: the first captures a node's local response to changes in its immediate neighborhood (S_i, I_i), and the second captures the propagation to distant nodes ($\Gamma(l)$, $P(G)$). The full impact of a perturbation, as captured by the cascade size C_i [41–47], is a combination of these two. Indeed, we can show that (Sec. S.V)

$$C_i \sim k_i^{\omega} \quad (17)$$

where

$$\omega = \frac{\beta + \varphi}{\beta + 1}, \quad (18)$$

which, like all the previously predicted exponents, is intrinsic to the system's dynamics. The dependence of C_i on the local impact (ϕ) and the propagation (β), gives rise to four classes of behavior (Fig. 4b1 - b4). For example, for $\mathcal{B}$, a conservative system ($\beta = 0$) with uniform local impact ($\phi = 0$), (18) predicts $\omega = 0$, indicating that C_i is independent of k_i, and hence $P(C)$ is bounded independently of the nature of $P(k)$ (Figs. 1e1 and 4b3). For $\mathcal{BD}$ we have a conservative system ($\beta = 0$) with heterogeneous local impact ($\phi = 3/2$), predicting $\omega = \phi = 3/2$ (Fig. 4b4). As C_i scales with k_i, we predict heterogeneous cascades in which $P(C)$ is determined by $P(k)$, being fat-tailed if $P(k)$ is fat-tailed (Fig. 1e2). The cascade heterogeneity is driven by the *local dynamics* through the heterogeneous local impact, hence $\omega = \phi$ and $P(C) \sim P(I)$. Regulatory dynamics ($\mathcal{R}$) is characterized by uniform local impact ($\phi = 0$), and dissipative dynamics ($\beta = 1$), having $\omega = 1/2$, predicting heterogeneous cascades (Figs. 1e3 and 4b1). As opposed to $\mathcal{BD}$, the cascade heterogeneity is a consequence of the propagation dynamics (β), rather than the local impact. This explains the surprising disparity between the local and the global behavior observed for $\mathcal{R}$: while $P(I)$ is bounded (Fig. 1b3), namely all nodes have comparable impact on their immediate neighbors, $P(C)$ could be fat-tailed (Fig. 1e3). Finally, the heterogeneous local impact ($\phi = 1$) of $\mathcal{E}$, coupled with the dissipative dynamics ($\beta = 1$) leads to heterogeneous cascades with $\omega = 1$ (18) (Figs. 1e4 and 4b2). For scale-free networks we can also predict the specific form of $P(C)$ (Sec. S.VII.E), in perfect agreement with the simulations (Fig 1e2 - e4, solid lines).

V. Dynamical Universality from Experimental Data

In many systems of practical importance the analytical form of the dynamics is unknown, hence we cannot predict the system's behavior from (1). Yet, the link we established between the universal exponents δ, ϕ, β and ω, and the macroscopically accessible $P(S)$, $P(I)$, $P(G)$ and $P(C)$ distributions allows us to determine a system's universality class even without knowing the analytical formulation of its dynamics. To demonstrate this we collected experimental data pertaining to social and biological systems, allowing us to show how to determine their dynamical universality class.

Human Dynamics

We used the temporal activity pattern of a user during email communication as a proxy for human dynamics, where $x_i(t)$ represents the number of emails sent by user i during a six hour interval [48]. We calculated $G_{ij} = \langle x_i x_j \rangle / \langle x_i^2 \rangle$ for each user pair (Sec. S.VIII.A). In Fig. 5a1 - b1 we show the stability and impact vs. k_i, finding that for large k_i, $S_i \sim k_i^\delta$ and $I_i \sim k_i^\varphi$ as predicted in Eqs. (10) and (11), with $\delta = 2.4 \pm 0.2$ and $\varphi = 2.1 \pm 0.1$. As $\delta > 0$ and $\varphi > 0$ this represents heterogeneous stability and impact, for which we expect $P(S)$ and $P(I)$ to be fat-tailed (Fig. 5a2 - b2). We also measured $P(G)$, finding $\nu = 2.0 \pm 0.1$ (Fig. 5c2), predicting that the dynamics is conservative ($\beta = 0$), independently confirmed by the non-decaying $\Gamma(l)$ (Fig. 5c1). The empirically obtained values for φ and β allow us to predict that $\omega = 2.1$ (18), leading to heterogeneous cascades. The cascade heterogeneity is driven by the local dynamics ($\varphi > 0$, $\beta = 0$), and hence we expect that $P(C) \sim P(I)$, confirmed by the empirical results. We also predict the precise form of $P(S)$, $P(I)$ and $P(C)$ (solid lines) from the empirically measured scale-free $P(k)$ ($\gamma = 2.0$), finding an excellent agreement with the empirical results (Sec. S.VII.E).

Cellular dynamics

We used high throughput microarray data collected for *S. cerevisiae*, to measure the impact of 55 genetically perturbed genes on the remaining 6, 222 genes [49]. In this system, not only is the dynamics unknown, but we also lack an accurate map of the underlying physical interactions. Still, we can directly measure the distributions $P(S)$, $P(I)$, $P(G)$ and $P(C)$ (Sec. S.VIII.B). We find that while $P(S)$ is bounded, $P(I)$ is fat-tailed, suggesting that expression patterns are described by uniform stability and heterogeneous local impact (Fig. 5e - f). The correlation distribution follows (15) with $\nu = 2.0 \pm 0.1$ (Fig. 5g), predicting a conservative dynamics with $\beta = 0$. The heterogeneous local impact ($\varphi > 0$) together with the conservative dynamics ($\beta = 0$) predict $\omega > 0$ in (18), hence $P(C)$ describes heterogeneous cascades, as observed in Fig. 5h. Since $\beta = 0$ the cascade heterogeneity is governed by the local impact ($\omega = \varphi$), as supported by the fact that $P(C) \sim P(I)$. Taken together the two systems indicate that we can obtain the relevant dynamical class from the direct measurement of the system's dynamical response to perturbations.

VI. Summary and Outlook

Predicting the *behavior* of a complex system requires a joint quantitative description of the system's structure and dynamics. Much of the advances obtained to date were system dependent, suggesting that each dynamical system requires its unique suite of analytical and numerical tools to understand its behavior [14–16, 27, 28]. Here we developed a self-consistent formalism that defies this wisdom. We bridge topology and dynamics, predicting that a complex system's response to perturbations is driven by a small number of universal characteristics. This universality defines a minimal set of *relevant exponents*, δ, φ, ν, β and ω, which can be all uniquely derived from the dynamical rules that govern the system. Our demonstration of the existence of distinct dynamical universality classes offers new avenues for future empirical and theoretical work. On the empirical side, the small number of possible dynamical behaviors suggests that the direct measurement of $P(G)$, $P(S)$, $P(I)$, $P(C)$

and $\Gamma(l)$ could provide crucial insights on the system's dynamics, potentially allowing us to infer the leading terms of the dynamical functions $f(x_i)$ and $g(x_j)$ (6) from empirical data. This would allow to develop an effective continuum theory for systems whose dynamics remains unknown, drawing a connection between the empirically accessible quantities and the system's mechanistic description.

The fact that our formalism also works for the two experimental systems indicates that the conclusions we derived from Eq. (1) are rather general, applying to systems of yet unknown dynamics as well. This is not unexpected: our main finding is that no matter what is the detailed structure of $W(x_i)$ and $Q(x_i, x_j)$, the number of distinct dynamical patterns Eq. (1) can display is finite, governed by the leading terms of the Laurent expansions of Eqs. (7) and (8). Hence any dynamical system that follows (1), independent of the precise form of $W(x_i)$ and $Q(x_i, x_j)$, should be classifiable into one of the predicted universality classes.

That being said, further work is needed to generalize our approach to non-stationary phenomena and to dynamical processes that cannot be cast in the form (1). Such a program could either place non-stationary systems within the framework developed above or could unlock an even richer set of dynamical characteristics. For example, threshold models used in social networks [50] and Boolean network models [51], whose node activities are discrete, are not obviously accounted for by (1). Aided by the increasing availability of empirical data, this approach could bring us closer to the construction of a powerful dynamical theory of complex systems, impacting numerous disciplines, from cell biology to human dynamics.

Supplementary Material

Refer to Web version on PubMed Central for supplementary material.

Acknowledgments

References

1. Caldarelli, G. Scale-free networks: complex webs in nature and technology. Oxfrod University Press; New York: 2007.

2. Drogovtsev, SN.; Mendez, JFF. Evolution of networks: from biological nets to the Internet and WWW. Oxford University Press; Oxford: 2003.

3. Strogatz SH. Exploring complex networks. Nature. 2001; 410:268–276. [PubMed: 11258382]

4. Helbing, D.; Jost, J.; Kantz, H., editors. Networks and Heterogeneous Media (NHM). Vol. 3. AIMS; Springfield, MO., USA: 2008. Networks and complexity; p. 185-411.

5. Newman, MEJ. Networks - an introduction. Oxford University Press; New York: 2010.

6. Pastor-Satorras, R.; Vespignani, A. Evolution and structure of the Internet: A statistical physics approach. Cambridge University Press; Cambridge, U.K.: 2004.

7. Palla G, Derényi I, Farkas I, Vicsek T. Uncovering the overlapping community structure of complex networks in nature and society. Nature. 2005; 435:814–818. [PubMed: 15944704]

8. Cohen, R.; Havlin, S. Complex networks: Structure, robustness and function. Cambridge University Press; New York, NY: 2010.

9. Watts DJ, Strogatz SH. Collective dynamics of 'small-world' networks. Nature. 1998; 393:440–442. [PubMed: 9623998]

10. Barabási AL, Albert R. Emergence of scaling in random networks. Science. 1999; 286:509–512. [PubMed: 10521342]

11. Girvan M, Newman MEJ. Community structure in social and biological networks. Proc Natl Acad Sci US. 2002; 99:7821–26.

12. Newman MEJ. Assortative mixing in networks. Phys Rev Lett. 2002; 89:208701–4. [PubMed: 12443515]

13. Pastor-Satorras R, Vázquez A, Vespignani A. Dynamical and correlation properties of the Internet. Phys Rev Lett. 2001; 87:258701. [PubMed: 11736611]

14. Dorogovtsev SN, Goltsev AV. Critical phenomena in complex networks. Rev Mod Phys. 2008; 80:1275–1335.

15. Barrat, A.; Barthélemy, M.; Vespignani, A. Dynamical Processes on Complex Networks. Cambridge University Press; Cambridge: 2008.

16. Holter NS, Maritan A, Cieplak M, Fedoroff NV, Banavar JR. Dynamic modeling of gene expression data. Proc Natl Acad Sci US. 2001; 98:1693–1698.

17. Strogatz SH. From Kuramoto to Crawford: exploring the onset of synchronization in populations of coupled oscillators. Physica D. 2000; 143:1–20.

18. Arenas A, Díaz-Guilera A, Kurths J, Moreno Y, Zhou C. Synchronization in complex networks. Physics Reports. 2008; 469:93–153.

19. Lloyd AL, May RM. How viruses spread among computers and people. 2001; 292:1316–1317.

20. Barthélémy M, Barrat A, Pastor-Satorras R, Vespignany A. Velocity and hierarchical spread of epidemic outbreaks in scale-free networks. Phys Rev Lett. 2004; 92:178701. [PubMed: 15169200]

21. Barthélémy M, Barrat A, Pastor-Satorras R, Vespignany A. Dynamical patterns of epidemic outbreaks in complex heterogeneous networks. J Theor Bio. 2005; 235:275–288. [PubMed: 15862595]

22. de Aguiar MAM, Bar-Yam Y. Spectral analysis and the dynamic response of complex networks. Phys Rev E. 2000; 71:016106.

23. Pastor-Satorras R, Vespignani A. Epidemic spreading in scale-free networks. Phys Rev Lett. 2001; 86:3200–3203. [PubMed: 11290142]

24. Hufnagel L, Brockmann D, Geisel T. Forecast and control of epidemics in a globalized world. Proc Natl Acad Sci US. 2004; 101:15124–9.

25. Dodds PS, Watts DJ. A generalized model of social and biological contagion. Journal of Theoretical Biology. 2005; 232:587–604. [PubMed: 15588638]

26. Voit, EO. Computational Analysis of Biochemical Systems. Cambridge University Press; New York, NY: 2000.

27. Maslov S, Ispolatov I. Propagation of large concentration changes in reversible protein-binding networks. Proc Natl Acad Sci USA. 2007; 104:13655–60. [PubMed: 17699619]

28. Maslov S, Ispolatov I. Spreading out of perturbations in reversible reaction networks. New Journal of Physics. 2007; 9:273–283. [PubMed: 18046464]

29. Yan KK, Walker D, Maslov S. Fluctuations in Mass-Action Equilibrium of Protein Binding Networks. Phys Rev Lett. 2008; 101:268102–6. [PubMed: 19437675]

30. Gardiner, CW. Handbook of Stochastic Methods. Springer-Verlag; Berlin: 2004.

31. Novozhilov AS, Karev GP, Koonin EV. Biological applications of the theory of birth-and-death processes. Briefings in Bioinformatics. 2006; 7:70–85. [PubMed: 16761366]

32. Hayes, JF.; Ganesh Babu, TVJ. Modeling and Analysis of Telecommunications Networks. John Wiley & Sons, Inc.; Hoboken, NJ, USA: 2004.

33. Alon, U. An Introduction to Systems Biology: Design Principles of Biological Circuits. Chapman & Hall; London, U.K.: 2006.

34. Karlebach G, Shamir R. Modelling and analysis of gene regulatory networks. Nature Reviews. 2008; 9:770–780.

35. Kuznetsov VA, Knott GD, Bonner RF. General statistics of stochastic process of gene expression in eukaryotic cells. Genetics. 2002; 161:1321–1332. [PubMed: 12136033]

36. Hoyle DC, Rattray M, Jupp R, Brass A. Making sense of microarray data distributions. Bioinformatics. 2002; 18:576–584. [PubMed: 12016055]

37. Harris EE, Sawhill B, Wuensche A, Kauffman S. A model of transcriptional regulatory networks based on biases in the observed regulation rules. Complexity. 2003; 7(4):23–40.

38. Furusawa C, Kaneko K. Zipf s law in gene expression. Phys Rev Lett. 2003; 90:088102. [PubMed: 12633463]

39. Lu T, Costello CM, Croucher PJP, Häsler R, Deuschl G, Schreiber S. Can Zipf's law be adapted to normalize microarrays? BMC Bioinformatics. 2005; 6:37–49. [PubMed: 15727680]

40. Alamaas E, Kovács B, Vicsek T, Oltvai ZN, Barabási AL. Global organization of metabolic fluxes in the bacterium *Escherichia coli*. Nature. 2004; 427:839–843. [PubMed: 14985762]

41. Eguíluz VM, Chialvo DR, Cecchi GA, Baliki M, Apkarian AV. Scale-free brain functional networks. Phys Rev Lett. 2005; 94:018102. [PubMed: 15698136]

42. Leskovec J, Singh A, Kleinberg J. Patterns of influence in a recommendation network. Lecture Notes in Computer Science. 2006; 3918:380.

43. Leskovec J, Mcglohon M, Faloutsos C, Glance N, Hurst M. Patterns of cascading behavior in large blog graphs. Proceeding of the SIAM International Conference on Data Mining. 2007:551–556.

44. Meeyoung, C.; Mislove, A.; A, B.; Gummadi, K. Proceedings of the first workshop on Online social networks. ACM; New York, NY, USA: 2008. Characterizing social cascades in flickr; p. 13-18.WOSN '08

45. Crucitti P, Latora V, Marchiori M. Model for cascading failures in complex networks. Phys Rev E. 2004; 69:045104.

46. Dobson I, Carreras BA, Lynch VE, Newman DE. Complex systems analysis of series of blackouts: Cascading failure, critical points, and self-organization. Chaos. 2007; 17:026103. [PubMed: 17614690]

47. Kauffman S. The ensemble approach to understand genetic regulatory networks. Physica A. 2004; 340:733–740.

48. Eckmann JP, Moses E, Sergi D. Entropy of dialogues creates coherent structures in e-mail traffic. Proc Natl Acad Sci US. 2004; 101:14333–7.

49. Chua G, et al. Identifying transcription factor functions and targets by phenotypic activation. Proc Natl Acad Sci US. 2006; 103:12045–50.

50. Granovetter M. Threshold models of collective behavior. The Americn journal of Sociology. 2002; 83(6):1420–43.

51. Bornholdt S. Boolean network models of cellular regulation: prospects and limitations. J R Soc Interface. 2008; 5:S85–S94. [PubMed: 18508746]

52. Yu H, et al. High-quality binary protein interaction map of the yeast interactome network. Science. 2008; 322:104–110. [PubMed: 18719252]

53. Milo R, Shen-Orr S, Itzkovitz S, Kashtan N, Chklovskii D, Alon U. Network motifs: Simple building blocks of complex networks. Science. 2002; 298:824–827. [PubMed: 12399590]

54. Milojevi S. Power law distributions in information science: Making the case for logarithmic binning. Journal of the American Society for Information Science and Technology. 2010; 61(12): 2417–2425.
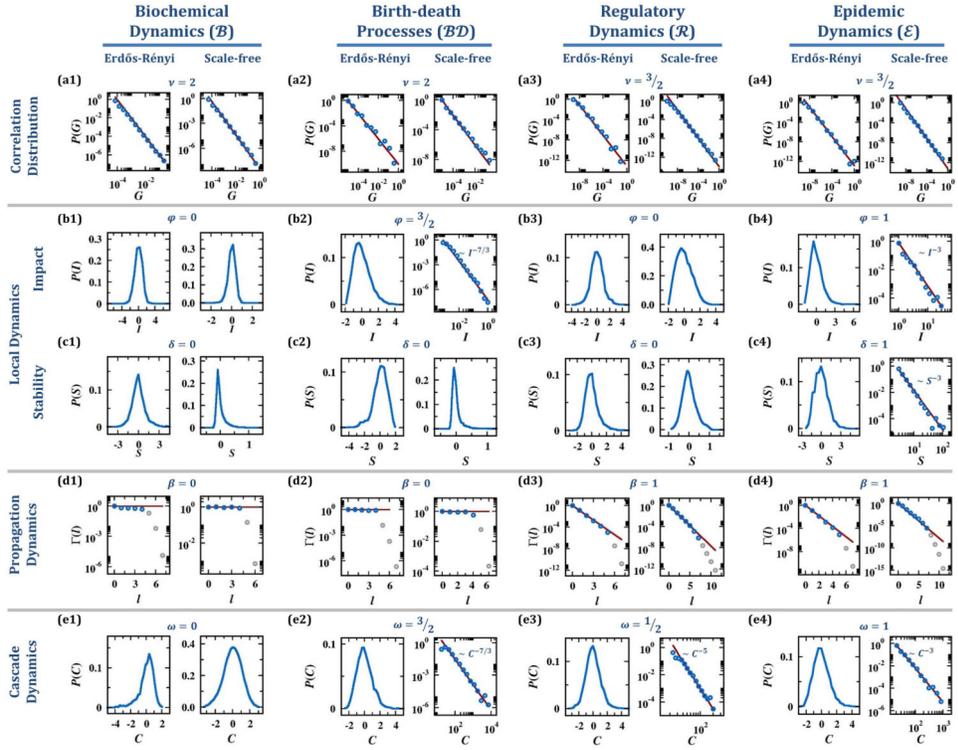
Fig. 1. The observed dynamical behavior of model systems

We used the response of a system to external perturbations to determine the five functions that capture the local dynamics between neighbors, the propagation of perturbations to more distant nodes and the global cascades, using numerical simulations. (a1) - (a4) For all four models we find that $P(G) \sim G^{-\nu}$, independent of the network topology (Erd s-Rényi, scale-free or empirical). For $\mathcal{B}$ and $\mathcal{BD}$ $\nu = 2$ and for $\mathcal{R}$ and ε $\nu = 3/2$, in perfect agreement with the prediction of (15) and (16) (solid red lines). (b1) - (c4) The impact and stability distributions, $P(I)$ and $P(S)$, show diverse behavior: for $\mathcal{B}$ and $\mathcal{R}$ both $P(I)$ and $P(S)$ are bounded independently of $P(k)$, for $\mathcal{BD}$ $P(I)$ is fat-tailed on a scale-free network while $P(S)$ is bounded, and for ε both are fat-tailed. For scale-free networks ($P(k) \sim k^{-\gamma}$) we can predict $P(S)$ and $P(I)$ using $P(K = k^y) \sim K^{-Y}$, where $Y = (\gamma + y - 1)/y$ (solid red lines, Sec. S.VII.E), in agreement with simulations. (d1) - (d4) The propagation of perturbations is captured by the correlation function $\Gamma(l)$ (5): $\mathcal{B}$ and $\mathcal{BD}$ exhibit conservative propagation, as perturbations penetrate the network without loss; $\mathcal{R}$ and ε exhibit dissipative propagation, as perturbations decay exponentially with l. The theoretical prediction (14) (solid red lines) is in agreement with the numerical results. For $l > \langle l \rangle$ the effect of the perturbation drops sharply, as the propagation has exhausted most nodes in the network (gray circles), and Eq. (14) is no longer valid (see Sec. S.IV where we analytically predict the behavior of $\Gamma(l)$ for $l > \langle l \rangle$). (e1) - (e4) The global impact of a perturbation is captured by the cascade size. While in three of the models ($\mathcal{BD}$, $\mathcal{R}$, and ε $P(C)$ is driven by $P(k)$, being consequently fat-tailed or bounded, $\mathcal{B}$ has a bounded $P(C)$ independently of the network topology. The results are consistent with the theoretical prediction of (17) and (18). The theoretical prediction for scale-free networks (solid red lines) is in agreement with the numerical results.
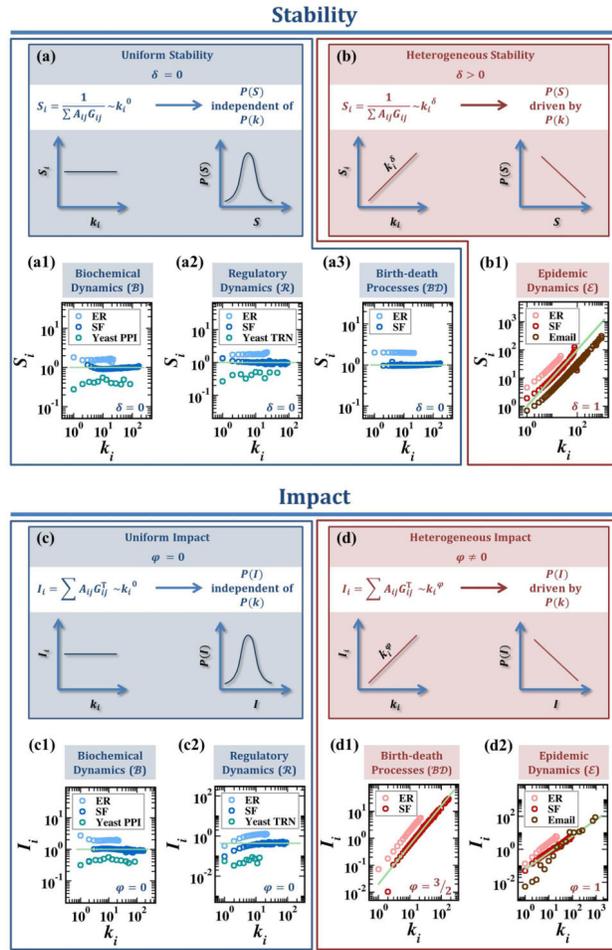
Fig. 2. Local dynamics: Stability and Impact

The *stability* S_i, characterizing a node's response to perturbations in its vicinity, features two dynamical universality classes. (a) *Uniform stability*: if $\delta = 0$ in (10), the stability is independent of the node's degree and $P(S)$ is bounded, regardless of the form of $P(k)$. As predicted, $\mathcal{B}$ (a1), $\mathcal{R}$ (a2) and $\mathcal{BD}$ (a3) belong to this class, featuring $S_i \sim k_i^0$. Hence regardless of whether the underlying network is random (ER), scale-free (SF) or an empirical network (yeast protein-protein interaction (PPI) network [52]; yeast transcriptional regulatory network (TRN) [53]; see Sec S.VII) $P(S)$ will be bounded (Fig. 1c1 - c3). (b) *Heterogeneous stability*: if $\delta > 0$ in (10), S_i depends on k_i and $P(S)$ is driven by $P(k)$, being fat-tailed if $P(k)$ is fat-tailed. For $\mathcal{E}$ (b1) we predict $\delta = 1$ (solid green line), in agreement with results obtained for both model and empirical networks (Email [48]), indicating that $P(S) \sim P(k)$ (Fig. 1c4). Where appropriate, here and in what follows, we used logarithmic binning to display the scaling of S_i [54]. *Impact*, I_i, characterizes the influence of i on its immediate neighbors. (c) *Uniform impact*, observed for $\varphi = 0$ in (11), leads to a bounded $P(I)$. $\mathcal{B}$ (c1) and $\mathcal{R}$ (c2) belong to this class ($I_i \sim k_i^0$), a prediction supported by their bounded $P(I)$ (Fig. 1b1 and b3). (d) *Heterogeneous impact*, observed when $\varphi \neq 0$ in (11), for which $P(I)$ is driven by $P(k)$. For $\mathcal{BD}$ (d1) we predict $\varphi = 3/2$ and for $\mathcal{E}$ (d2) $\varphi = 1$, in perfect

agreement with the numerical results. As I_i depends on k_i in this class $P(I)$ is driven by $P(k)$ (Fig. 1b2 and b4).

Propagation Dynamics

(a)

$$g(f^{-1}(x)) \longrightarrow g(f^{-1}(x)) = \sum_{n=-\infty}^{\infty} b_m x^m \longrightarrow \Gamma(l) = e^{-\beta \alpha l}$$

(b) **Conservative Dynamics**

$$\beta = 0$$

$$\Gamma(l) = 1 \longrightarrow \begin{array}{c} P(G) \sim G^{-\nu} \\ \nu = 2 \end{array}$$

(c) **Dissipative Dynamics**

$$\beta > 0$$

$$\Gamma(l) = e^{-\alpha \beta l} \longrightarrow \begin{array}{c} P(G) \sim G^{-\nu} \\ 1 < \nu < 2 \end{array}$$
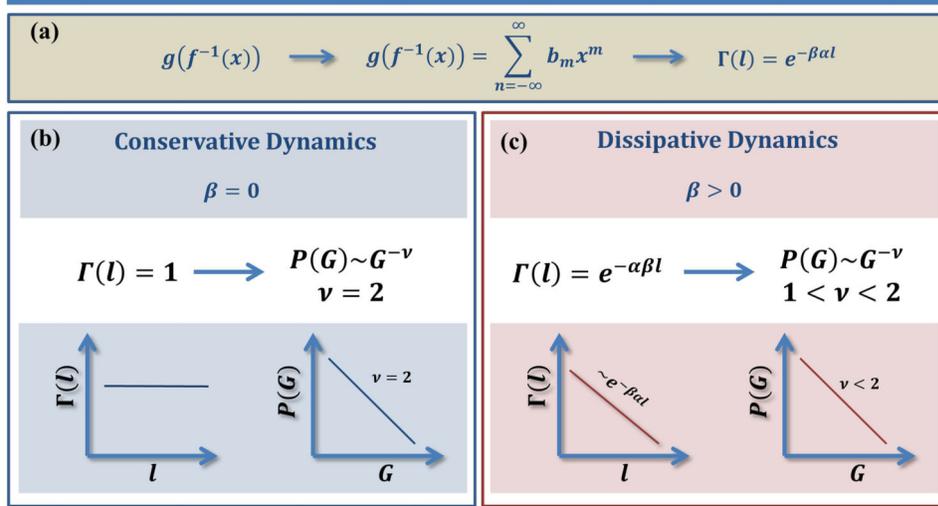
Fig. 3. Propagation of perturbations

(a) The propagation to distant nodes is governed by the structure of $g(f^{-1}(x))$ through the leading terms of (8), which determine the dissipation rate, β, in (14). (b) *Conservative dynamics*: If the leading term in (8) is m_0 0 we have $\beta = 0$, predicting a conservative propagation, in which perturbations penetrate the network without loss. As a result $\Gamma(l) = 1$ (14) and $P(G) \sim G^{-2}$ (15). We predict that $\mathcal{B}$ and $\mathcal{BD}$ are in this class, as confirmed by results in Figs. 1a1 - a2 and d1 - d2. (c) *Dissipative dynamics*: If the leading terms in (8) are $g(f^{-1}(x)) \sim b_0 + x^{m_1}$ we have $\beta = m_1 > 0$ in (14), leading to a dissipative propagation, in which perturbations decay exponentially with network distance. As a result $P(G) \sim G^{-\nu}$ (15) where $1 < \nu < 2$ (16). For $\mathcal{R}$ and $\mathcal{E}$ we predict $\beta = 1$ and hence $\nu = 3/2$, in perfect agreement with the results of Figs. 1a3 - a4 and d3 - d4.
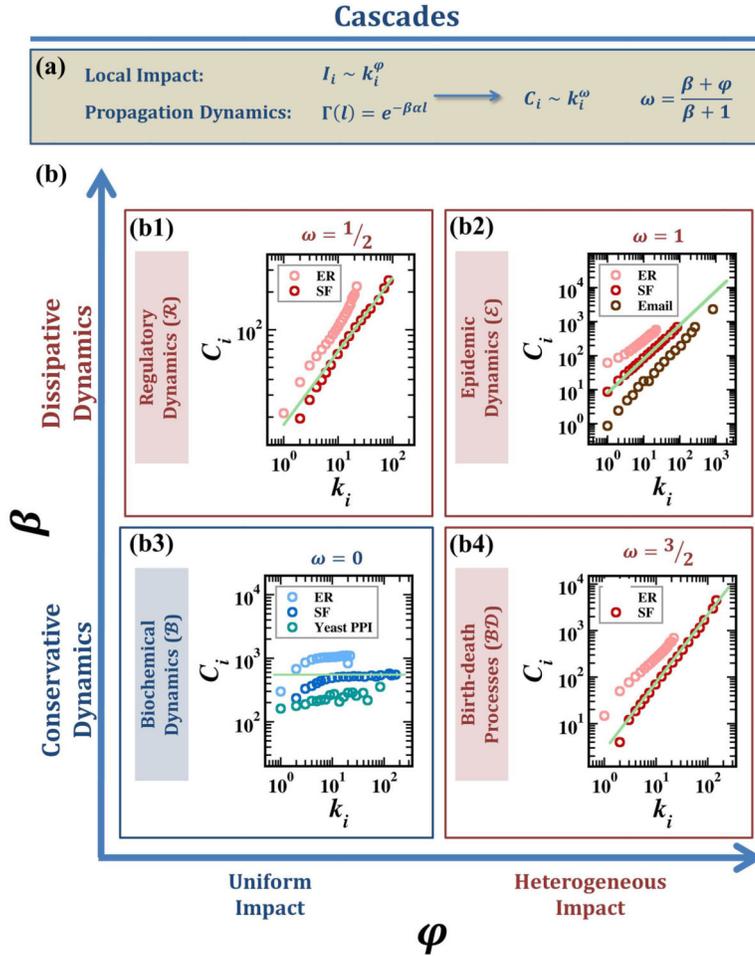
Fig. 4. Cascade sizes

(a) The cascade size is jointly driven by two mechanisms: the local impact of a node on its nearest neighbors (I_i) and the propagation from the neighbors to the rest of the network ($\Gamma(l)$). Hence $C_i \sim k_i^{\omega}$, where ω is determined by both ϕ and β (18). (b) Four classes of dynamical behavior emerge: (b1) For $\mathcal{R}$ we have $\beta = 1$ and $\phi = 0$, predicting $\omega = 1/2$, and hence heterogeneous cascades with $P(C)$ driven by $P(k)$, as confirmed by Fig. 1e3. Here the local dynamics is uniform (Fig. 1b3), and yet, remarkably, the global cascades can be heterogeneous due to the dissipative propagation ($\beta > 0$). (b2) For $\mathcal{E}$ we have $\beta = \phi = 1$, predicting $\omega = 1$, a heterogeneous cascade dynamics, as shown in Fig. 1e4. (b3) For $\mathcal{B}$ we have $\beta = \phi = 0$, and hence $\omega = 0$, predicting uniform cascades. Here even if $P(k)$ is fat-tailed, $P(C)$ will be bounded, so that the dynamical behavior is largely independent of the topological heterogeneity (Fig. 1e1). (b4) For $\mathcal{BD}$ we have $\beta = 0$ and $\phi = 3/2$, predicting $\omega = 3/2$, a heterogeneous cascade dynamics, as shown in Fig. 1e2. The heterogeneity in this case, in which $\beta = 0$, is driven by the local dynamics and hence $P(C) \sim P(I)$ (Fig. 1b2).
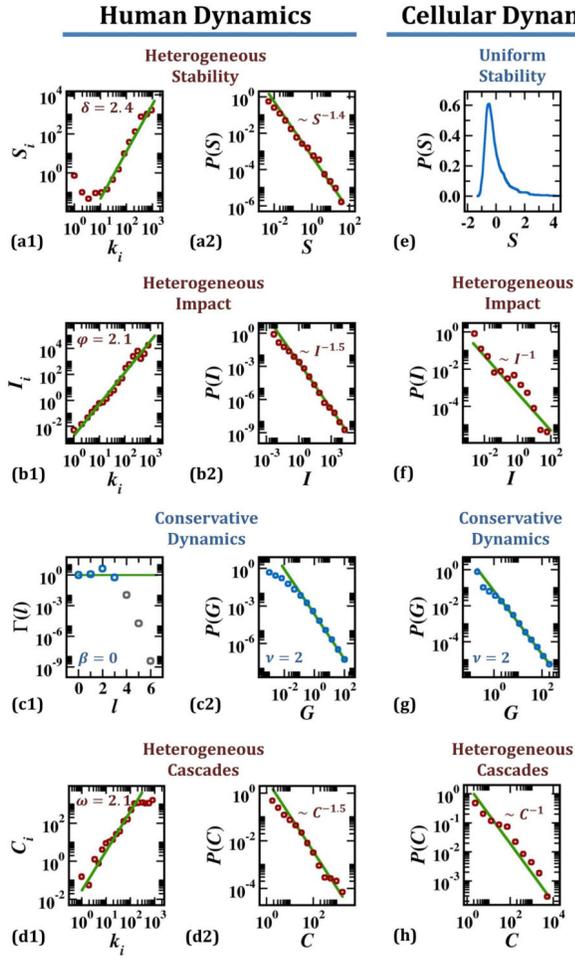
Fig. 5. Uncovering the dynamical universality class from empirical data

Human Dynamics: We constructed G_{ij} from the correlations in the usage patterns of users in an email network [48] (Sec. S.VIII.A). (a1) The stability vs. k_i follows $S_i \sim k_i^{\delta}$ with $\delta = 2.4 \pm 0.2$, predicting heterogeneous stability. (a2) As expected for heterogeneous stability, the system features a fat-tailed $P(S)$. (b1) - (b2) The local impact vs. k_i follows $I_i \sim k_i^{\varphi}$ with $\varphi = 2.1 \pm 0.1$, predicting heterogeneous impact with a fat-tailed $P(I)$. (c1) The correlation function $\Gamma(l)$ does not decay, indicating conservative dynamics. (c2) As expected for conservative dynamics, $P(G) \sim G^{-\nu}$ with $\nu = 2$. (d1) - (d2) From the measured β and φ we predict $\omega = 2.1$ in (17) and hence expect a fat-tailed $P(C)$. As $\beta = 0$ we also expect that $P(C) \sim P(I)$. Indeed, we find that $P(C) \sim C^{-1.5}$ and $P(I) \sim I^{-1.5}$, in agreement with the prediction for a scale-free network (Sec. S.VII.E). For large ki the cascades saturate due to the finite size of the network ($N = 2, 668$). *Cellular Dynamics*: To test our predictions for a biological system we collected perturbation data in which 55 yeast genes were perturbed, measuring their impact on the rest of the 6, 222 genes, giving rise to a 6, 222 × 55 correlation matrix, G_{ij} [49]. Lacking the wiring diagram we could not measure δ, φ, β and ω directly. Yet, we can identify the universality class by measuring $P(I)$, $P(S)$, $P(G)$ and $P(C)$, which do not require knowledge on the underlying topology (Sec. S.VIII.B). (e) $P(S)$ indicates uniform stability ($\delta = 0$); (f) $P(I)$ indicates heterogeneous impact ($\varphi \neq 0$), in which $P(I) \sim I^{-1}$; (g)

$P(G)$ has $\nu = 2$, indicating conservative dynamics ($\beta = 0$); (h) From the inferred values of φ and β we predict $\omega > 0$, foreseeing heterogeneous cascades, a prediction supported by the fat-tailed $P(C) \sim C^{-1}$. As $\beta = 0$, we expect that cascade heterogeneity is driven by the local dynamics, also supported by the fact that $P(C) \sim P(I)$.

Table I

Dynamical models

Summary of four frequently explored network based dynamical models analyzed in the paper. Biochemical dynamics ($\mathcal{B}$): The dynamics of protein-protein interactions is captured by mass-action kinetics (MAK) [26–29]. In the model proteins are produced at rate F, degraded at rate B and generate hetero-dimers at rate $\mathcal{R}$ (see Sec. S.VII.C, where we also account for the hetero-dimer dissociation). Birth-death processes ($\mathcal{BD}$): This equation, emerging in queuing theory [32], population dynamics [30, 31] and biology [26], describes the population density at site i. The first term describes the local population dynamics and the second term describes the coupling between adjacent sites. Here we set $b = 2$, representing pairwise depletion, and $a = 1$, describing a linear flow from i's neighboring sites (see Sec. S.VII.D, where we solve for a general choice of a and b). Regulatory dynamics ($\mathcal{R}$): The dynamics of gene regulation is captured by the Michaelis-Menten (MM) equation [33, 34]. Here the parameter h is the Hill coefficient, which we set to $h = 1$ (see Sec. S.VII.B, where we solve for general h). Epidemic dynamics ($\mathcal{E}$): The spread of infectious diseases/ideas is captured by the susceptible-infected-susceptible (SIS) model [23–25] (Sec. S.VII.A). For each of the four models the table lists the associated dynamical functions $W(x_i)$ and $Q(x_i, x_j)$ in Eq. (1) and $f(x)$ and $g(x)$ as defined in Eq. (6), the exponents δ, φ and β determined from the Laurent expansions (7) and (8), and the exponents ν (16) and ω (18), derived from δ, φ and β.

Dynamics	Model	Rate Equation	$W(x_i)$	$Q(x_i, x_j)$	$f(x)$	$g(x)$	δ	φ	β	ν	ω
Biochemical ($\mathcal{B}$)	MAK	$\dfrac{dx_i}{dt}=F-Bx_i-\sum_{j=1}^{N}A_{ij}Rx_ix_j$	$W(x_i)=F-Bx_i$	$Q(x_i,x_j)=-Rx_ix_j$	$f(x)=\dfrac{Rx}{F-Bx}$	$g(x)=x$	0	0	0	2	0
Birth-death processes ($\mathcal{BD}$)	BDP	$\dfrac{dx_i}{dt}=-Bx_i^b+\sum_{j=1}^{N}A_{ij}Rx_j^a$	$W(x_i)=-Bx_i^b$	$Q(x_i,x_j)=Rx_j^a$	$f(x)=\dfrac{R}{Bx^b}$	$g(x)=x^a$	0	$\dfrac{3}{2}$	0	2	$\dfrac{3}{2}$
Regulatory ($\mathcal{R}$)	MM	$\dfrac{dx_i}{dt}=-Bx_i+\sum_{j=1}^{N}A_{ij}R\dfrac{x_j^h}{1+x_j^h}$	$W(x_i)=-Bx_i$	$Q(x_i,x_j)=R\dfrac{x_j^h}{1+x_j^h}$	$f(x)=\dfrac{R}{Bx}$	$g(x)=\dfrac{x^h}{1+x^h}$	0	0	1	$\dfrac{3}{2}$	$\dfrac{1}{2}$
Epidemic ($\mathcal{E}$)	SIS	$\dfrac{dx_i}{dt}=-Bx_i+\sum_{j=1}^{N}A_{ij}R(1-x_i)x_j$	$W(x_i)=-Bx_i$	$Q(x_i,x_j)=R(1-x_i)x_j$	$f(x)=\dfrac{R(1-x)}{Bx}$	$g(x)=x$	1	1	1	$\dfrac{3}{2}$	1